İSTANBUL UNIVERSITY CERRAHPAŞA

ORIGINAL ARTICLE
Electrica 2025; 25: 1-14

Design of a Dual-Layer Capacity Configuration Model for Hybrid Energy Storage in Distribution Networks With Photovoltaic Power Sources

Xinping Huang[1], Decao Xu[2], Xuwu Qin[2], Xin Tao[2]

[1]State Grid Jibei Electric Power Beijing Transmission and Transformation Co., Ltd, Beijing, 100052, China
[2]State Grid Qinghai Electric Power Company, Qinghai Xining 810008, China

Cite this article as: X. Huang, D. Xu, X. Qin and X. Tao, "Design of a dual-layer capacity configuration model for hybrid energy storage in distribution networks with photovoltaic power sources," *Electrica*, 25, 0038, 2025. doi: 10.5152/electrica.2025.25038.

WHAT IS ALREADY KNOWN ON THIS TOPIC?

- *Existing research cannot decouple grid level economic goals from energy storage level operation constraints.*

WHAT THIS STUDY ADDS ON THIS TOPIC?

- *A novel dual layer capacity configuration model was proposed, which integrates photovoltaic power generation with lithium battery/supercapacitor hybrid energy storage systems.*
- *Improved system stability, improved response time, and increased economic returns under dynamic pricing mechanisms.*

Corresponding author's: Xinping Huang

E-mail:
Beijing202501@163.com

Received: March 10, 2025

Revision Requested: April 14, 2025

Last Revision Received: May 15, 2025

Accepted: May 26, 2025

Publication Date: November 28, 2025

DOI: 10.5152/electrica.2025.25038

ABSTRACT

The traditional distribution network has significant shortcomings in terms of distributed power access capability, automation level, and operational efficiency, making it difficult to meet the development needs of modern power systems. To this end, an innovative photovoltaic power (PP) and hybrid energy storage (ES) collaborative configuration model is proposed, which significantly improves the performance and economy of the distribution network by introducing a lithium battery super-capacitor hybrid ES system and a double-layer capacity optimization framework. This model adopts a dynamic service pricing mechanism in the upper level optimization to minimize the operating costs of the power grid. In the lower level optimization, the dynamic allocation of ES charging and discharging power is used to achieve the lowest operating costs of the PP station, and efficient decision-making is achieved using the IBM ILOG CPLEX Optimization Studio (CPLEX) solver. The experimental results show that the model achieves charging efficiencies of 90.1% and 92.3%, discharge efficiencies of 91.2% and 93.5%, and response times of 2.9 seconds and 3.1 seconds, respectively, in the tests of A and B locations. The performance is significantly better than traditional pumped storage and single ES schemes. Meanwhile, the output power curve of the model exhibits minimal fluctuations, effectively suppressing the intermittent effects of PP generation. Under both dynamic and fixed electricity pricing mechanisms, the model can intelligently guide ES to discharge at full power during peak load periods. The peak valley difference under dynamic electricity pricing is reduced by 219.8 kW, and the net income is increased to 112987.1 yuan, which is 42.9% higher than the fixed electricity pricing mechanism. Through the collaborative optimization of photovoltaic-hybrid ES and double-layer capacity configuration, the study not only solves the stability and economic problems of the distribution network but also provides a reliable technical solution for the high proportion of new energy access.

***Index Terms*—**Distribution network, dual-layer capacity configuration, electricity pricing mechanism, hybrid energy storage, photovoltaic power supply

I. INTRODUCTION

During the evolution of power systems, the conventional distribution network acts as a crucial link between power generation and consumption, responsible for transmitting and distributing electrical energy. However, advancements in the economy and society, along with changes in energy structures, are posing numerous obstacles to traditional distribution networks. On the one hand, the rapid advancement of urbanization has brought about a significant increase in population density and a sharp expansion of electricity demand, which has led to a continuous rise in the load of the distribution network and increasing operational pressure. At the same time, people's expectations for power supply reliability and requirements for power quality are also increasing. Any power interruption or voltage fluctuation may have a significant impact on daily life, industrial production, and even national security. On the other hand, traditional distribution networks have long relied on fossil fuels as the main source of electricity, which not only leads to serious environmental pollution problems such as greenhouse gas emissions exacerbating global warming but also accelerates the depletion of limited fossil resources, threatening

energy security and sustainable development. On a global scale, green and low-carbon have become the main theme of the times, and worldwide governments have implemented policies aimed at fostering the advancement and use of renewable energy sources while minimizing reliance on fossil fuels [1]. To address these challenges, photovoltaic power (PP) sources are increasingly being introduced into the distribution network as a clean and renewable form of energy. Amir et al. devised a smart energy management approach for electric vehicle charging stations, leveraging photovoltaic technology. By examining real-time weather and load demand information, the scheme optimized PP generation and grid power utilization at electric vehicle charging stations, and its effectiveness was confirmed through simulation analysis [2]. Gupta et al. created a particle swarm optimization-based model to identify the best spot for charging electric vehicles within a solar photovoltaic-powered microgrid. Their experimental findings demonstrated that the model could decrease daily allocation losses by an additional 8% [3]. Liu et al. introduced a forecasting technique utilizing a combination of Convolutional Neural Networks (CNN) and bidirectional Long Short-Term Memory (LSTM) to tackle the problem of energy imbalance in distribution networks. The outcomes indicated that this method had significant effectiveness in solving the optimal energy scheduling problem of large-scale distributed generation access to distribution systems [4]. Anupong et al. introduced an innovative renewable energy technology leveraging photovoltaic cells in saltwater analysis, incorporating oxidation processes and deep learning methods. This approach is designed for seamless integration with the World Wide Web to enhance water usage control and monitoring. The research findings indicated that the proposed technology achieved an accuracy rate of 96%, a precision rate of 86%, and a recall rate of 76% [5]. Yang et al. proposed a comprehensive energy system model based on wind-solar battery hydrogen storage and conducted multi-objective optimization research on the coordination of comprehensive energy system configuration planning and operation strategy. The aim was to solve the problem of configuring and planning different energy storage (ES) time scales in wind-solar storage renewable integrated energy systems. The experimental results showed that by introducing hydrogen storage and hydrogen internal combustion engine power generation as part of the ES system, the configuration capacity of the battery was reduced. Meanwhile, hydrogen internal combustion engines had certain advantages over fuel cells in terms of cost and technological maturity, which not only reduced system costs but also achieved long-term ES [6]. Bhatti et al. proposed a design, optimization, and performance analysis scheme for a hybrid independent microgrid to solve the renewable energy generation problem of an industrial facility in Iraq. The experimental results showed that the system had the ability to significantly reduce carbon dioxide emissions, saving approximately 18 116 tons over a 30-year period, which contributed to achieving sustainability and environmental management goals [7].

While these studies have advanced the integration of renewable energy into power systems, several critical research gaps remain unaddressed. First, existing approaches predominantly focus on either photovoltaic generation or ES in isolation, failing to establish an integrated framework that simultaneously optimizes their dynamic interactions under real-world grid constraints. The work of Amir et al. [2] and Gupta et al. [3], while innovative in energy management, did not account for the temporal mismatches between photovoltaic (PV) output fluctuations and demand patterns. Second, current hybrid ES solutions like those proposed by Yang et al. [6] primarily addressed long-duration storage needs through hydrogen systems, overlooking the crucial short-timescale power regulation required for mitigating second-to-minute PV variability. Third, most optimization models adopt single-layer architectures that cannot decouple grid-level economic objectives from storage-level operational constraints—a limitation evident in Liu's predictive method [4] which lacked bidirectional coordination between market signals and physical system responses. These gaps collectively hinder the development of truly adaptive power distribution systems capable of maintaining stability amid increasing renewable penetration.

Based on this, the study proposes to incorporate hybrid ES technology into the introduction of PP sources, construct a configuration model for the power grid, and further optimize it. A systematic modeling approach was adopted in this process. The distribution network model was based on an improved IEEE 33 node system, using a branch power flow model and considering ± 5% voltage amplitude constraints and line capacity limitations. The PP supply was connected using the Active Power-Reactive Power (PQ) node modeling method, and maximum power tracking was achieved through the maximum power point tracking (MPPT) algorithm. The hybrid ES system adopted a DC bus parallel topology structure, in which the lithium-ion battery used the Thevenin equivalent circuit model to characterize its dynamic characteristics, and the super-capacitor used Resistor-Capacitor (RC) trapezoidal circuit model to accurately describe its fast charging and discharging behavior. In terms of system control architecture, a hierarchical control scheme was studied and designed: The bottom layer was a device-level Proportional-Integral (PI) regulator, the middle layer used a power divider with fuzzy logic control, and the upper layer was configured with an energy manager based on model predictive control. The innovation of this modeling method is reflected in three aspects: firstly, it fully considered the actual operating conditions of three-phase imbalance in the distribution network. Secondly, variable step size simulation technology was used to effectively handle dynamic processes at multiple time scales ranging from seconds to hours. Finally, the accuracy of the model was verified on the RT-LAB OP5600 hardware in the loop platform, with a sampling period set to 50 μ s to ensure simulation accuracy. In the subsequent optimization design, the upper level (UL) optimization adopted mixed-integer second-order cone programming to handle the discrete-continuous variable coupling problem, while the lower level (LL) optimization was based on an improved particle swarm algorithm to achieve an efficient solution. This systematic modeling method laid a reliable foundation for subsequent double-layer capacity optimization.

The main contribution of the research lies in: First, proposing a collaborative optimization method for PP sources and hybrid ES systems, which effectively smooths power fluctuations at different time scales through the complementary characteristics of lithium batteries and super-capacitors. Second, an innovative dual-layer capacity optimization architecture was designed, with the upper layer focusing on the economic operation of the power grid and the lower layer optimizing the scheduling of ES systems, establishing a collaborative optimization framework between market mechanisms and physical systems. Finally, an ES charging and discharging strategy based on dynamic service electricity prices was developed, providing a new solution for the economic and efficient operation of the distribution network. These innovations have significantly improved the stability and economy of the distribution network under high proportion renewable energy access conditions.

II. METHODS AND MATERIALS

A. Construction of Distribution Network Model Including Photovoltaic Power and Hybrid Energy Storage

In contemporary society, the demands placed on distribution network scheduling are escalating at an unprecedented rate. Traditional distribution networks that adopt centralized control methods have begun to face problems such as difficulty in meeting existing demands due to their low level of automation. As a system that converts solar energy into electrical energy, PP can reduce grid losses and improve energy utilization efficiency. Its structure is shown in Fig. 1.

Fig. 1 shows a distribution network power generation system with PP sources. From the figure, PP sources are mainly composed of solar panels, battery packs, inverters, and grid connection equipment. Hybrid ES is the combination of two or more different types of ES technologies to form a complete system, as shown in Fig. 2.

Fig. 2 shows a hybrid ES system. This system typically consists of electrochemical and physical ES systems, which are capable of smoothing out power fluctuations in the grid, particularly during the extensive integration of renewable energy. By storing and discharging electrical energy, these systems maintain the stable operation of the grid [8]. Consequently, integrating PP sources with hybrid ES can advance the development of smart grids and enhance the overall effectiveness and dependability of the power system. The output power of PP sources is predominantly influenced by environmental factors, such as light intensity and temperature variations, as illustrated in (1).

$$\begin{cases} I_{PV} = I_{sc}\left\{1 - C_1[\exp(\dfrac{V_{PV}}{C_2 V_{ocref}}) - 1]\right\} \\ S = 1000\text{W/m}^2 \qquad \text{T}=25^{\circ}\text{C} \end{cases} \tag{1}$$

Equation (1) represents the correlation between the PP source output current and its corresponding voltage. Among them, S means the intensity of light, T means the ambient temperature, I_{PV} represents the output current of the PP supply, V_{ocref} represents the open-circuit voltage, V_{PV} represents the output voltage, and I_{sc} represents the short-circuit current. C_1 and C_2 are undetermined coefficients. The specific calculation of the undetermined coefficients can be seen in (2).

$$\begin{cases} C_1 = (1 - \dfrac{I_{mpref}}{I_{scref}})\exp(-\dfrac{V_{mpref}}{C_2 V_{ocref}}) \\ C_2 = (\dfrac{V_{mpref}}{V_{ocref}} - 1)[\ln(1 - \dfrac{I_{mpref}}{I_{scref}})]^{-1} \end{cases} \tag{2}$$

In (2), V_{ocref} represents the voltage in an open-circuit state, I_{scref} represents the current in a short-circuit state, I_{mpref} means the current at maximum power, and V_{mpref} means the current at maximum power. Given the impact of environmental factors on the output power of PP sources, a solution to this challenge lies in employing the MPPT algorithm. This algorithm ensures that the PP source operates at its maximum electrical power output under all conditions, thus enhancing the overall system efficiency and energy yield, as demonstrated in (3).

$$\begin{cases} i_{pv}(z+1) = i_{pv}(z) + i_{pv}^{*}\, sign(p_{pv}(z) - p_{pv}(z-1)) \\ sign(x) = \begin{cases} 1 & x \geq 0 \\ -1 & x < 0 \end{cases} \end{cases} \tag{3}$$

Equation (3) is the perturbation observation method in MPPT. This method determines the direction of movement of the operating point by periodically applying small disturbances to the system and observing the direction of change in output power. If the power increases, the process continues to perturb in the same direction, and if the power decreases, it perturbs in the opposite direction. This iterative process ultimately stabilizes the system to operate near the maximum power point. In (3), $i_{pv}(z+1)$ represents the reference current at time $t+1$, and $i_{pv}(z)$ means the reference current at time t [9, 10]. i_{pv}^{*} represents current disturbance signal and p_{pv} represents power. Based on this, the basic parameters at any irradiation intensity and ambient temperature can be obtained, as shown in (4).

$$\begin{cases} I_{sc} = I_{scref}\dfrac{H_\theta}{H_{ref}}(1 + a\Delta T) \\ V_{oc} = V_{ocref}\ln(e + b\Delta H)(1 - c\Delta T) \\ I_{mp} = I_{mpref}\dfrac{H_\theta}{H_{ref}}(1 + a\Delta T) \\ V_{mp} = V_{mpref}\ln(e + b\Delta H)(1 - c\Delta T) \end{cases} \tag{4}$$

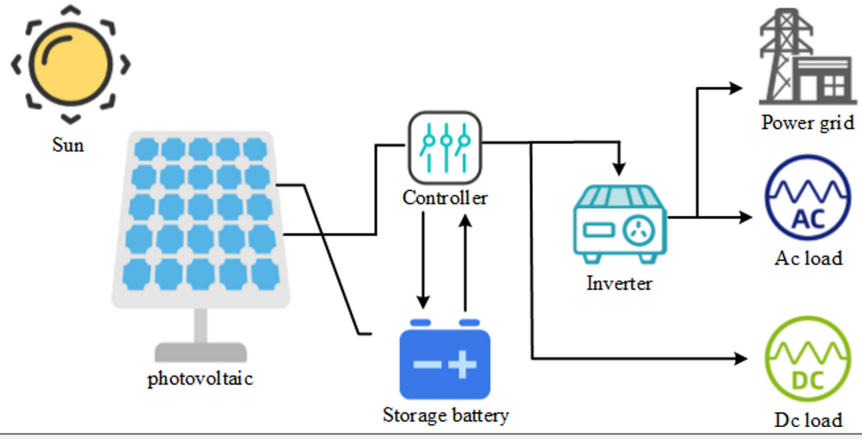

Fig. 1. Photovoltaic power generation system.

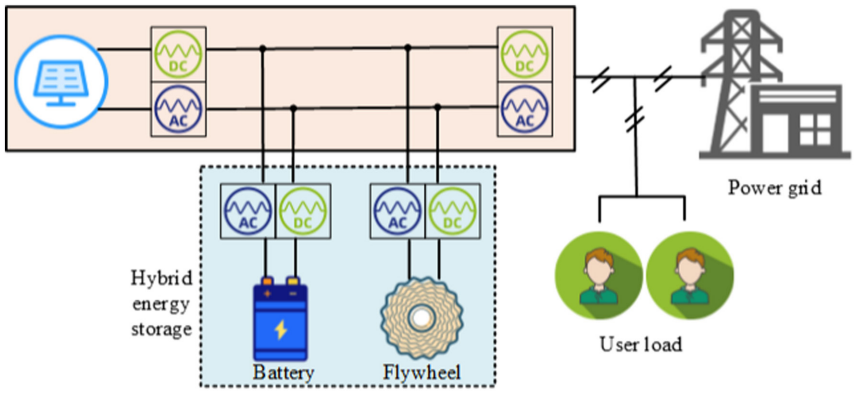

Fig. 2. Hybrid energy storage system.

In (4), ΔH represents the difference in light intensity and ΔT represents the difference in temperature. H_θ is the actual total light intensity received by the PP source. H_{ref} represents the light intensity under standard assumptions, that is, $H_{ref}=S=1000$ W/m^2. b is the correction coefficient representing light intensity. a and c are the correction coefficients representing temperature [11, 12]. Grounded on the above, the maximum power output of the PP source can be calculated, as shown in (5).

$$P_{mp}=P_{ref}\frac{H_\theta}{H_{ref}}(1+a\Delta T)\ln(e+b\Delta H)(1-c\Delta T) \tag{5}$$

In (5), P_{mp} represents the maximum output power. P_{ref} represents the rated power. Based on the above, a PP generation system model containing PP sources can be constructed. For the construction of hybrid ES system models, it is necessary to combine different types of ES technologies together [13, 14]. Taking into account both economic feasibility and technological sophistication comprehensively, a combination of lithium batteries and super-capacitors is selected as a new hybrid ES technology to jointly provide fast frequency regulation and voltage stability support for the power grid. Among them, the ES modeling of lithium batteries is shown in (6).

$$\begin{cases} \mathrm{SOC}=\dfrac{Q_{(t)}}{Q_\mathrm{N}} \\ \mathrm{SOC}_{\min}\le \mathrm{SOC}_{(t)}\le \mathrm{SOC}_{\max} \\ Q_{(t)}=Q_{(t-1)}+\Delta t P_{\mathrm{ESS}(t)} \\ 0\le P_{\mathrm{ESSc}(t)}\le P_{\mathrm{ESScmax}} \\ 0\le P_{\mathrm{ESSd}(t)}\le P_{\mathrm{ESSdmax}} \\ P_{\mathrm{ESSc}(t)}P_{\mathrm{ESSd}(t)}=0 \end{cases} \tag{6}$$

In (6), SOC represents the state of charge of the ES battery, $\mathrm{SOC}_{\min}$ represents the minimum value of the percentage of energy stored in the ES device, $\mathrm{SOC}_{\max}$ is the maximum value of the percentage of energy stored in the ES device, $Q(t)$ is the remaining capacity of the battery, and Q_N is the rated capacity of the battery for ES. Δt represents the time difference, $P_{\mathrm{ESS}}(t)$ represents the charging and discharging power, P_{ESScmax} is the maximum charging power, and P_{ESSdmax} is the maximum discharging power. In addition, the ES modeling of super-capacitors is shown in (7).

$$SOC_{sc}(t)=\begin{cases} SOC_{sc}(t-1)-\dfrac{\eta_{cv}\eta_{sc,ch}\int_0^{\varphi\Delta t}P_{sc}(t)\mathrm{d}t}{E_{sc,N}} & ,P_{sc}(t)\ge 0 \\ SOC_{sc}(t-1)-\dfrac{\eta_{cv}\int_0^{\varphi\Delta t}P_{sc}(t)\mathrm{d}t}{E_{sc,N}\eta_{sc,dis}} & ,P_{sc}(t)<0 \end{cases} \tag{7}$$

In (7), SOCsc (t) is the real-time state of charge of the super-capacitor, E_{sc},N represents the rated capacity of the super-capacitor, P_{sc} (t) represents the charging and discharging power of the super-capacitor, $\eta_{sc,ch}$ represents the charging efficiency of the super-capacitor, and $\eta_{sc,dis}$ represents the discharging efficiency of the super-capacitor. Due to the two configuration methods of ES systems in PP distribution networks, one is distributed, and the other is centralized. Considering the factors of later maintenance and repair, the study adopts a centralized ES configuration. Based on this, a distribution network model combining PP and hybrid ES can be constructed, as shown in Fig. 3.

Fig. 3 shows the distribution network structure with PP sources and hybrid ES systems. From the figure, PP is mainly used for power generation, while hybrid ES systems are composed of lithium batteries and super-capacitors. The introduction of these two modules can improve the traditional power grid, optimize energy configuration, and reduce power supply costs. It should be noted that the study adopts a centralized ES configuration, and the location selection of PP stations and ES systems is based on the following considerations: Firstly, the site is located at the end of the distribution network feeder to maximize the consumption of photovoltaic output. Secondly, by calculating the electrical distance, it can be ensured that the ES system is located in the vicinity of the weakest node in the power grid voltage support. This configuration method can not only avoid the coordination and control problems caused by distributed ES, but also effectively improve the power quality of local power grids. In addition, the hybrid ES system used by the research adopts a DC bus parallel topology structure, in which a lithium battery pack and a super-capacitor are connected in parallel to a common DC bus through a bidirectional DC/DC converter. Among them, lithium batteries serve as the main ES unit to undertake base load regulation and energy type applications, while super-capacitors serve as auxiliary units to compensate for high-frequency power fluctuations. This topology structure retains

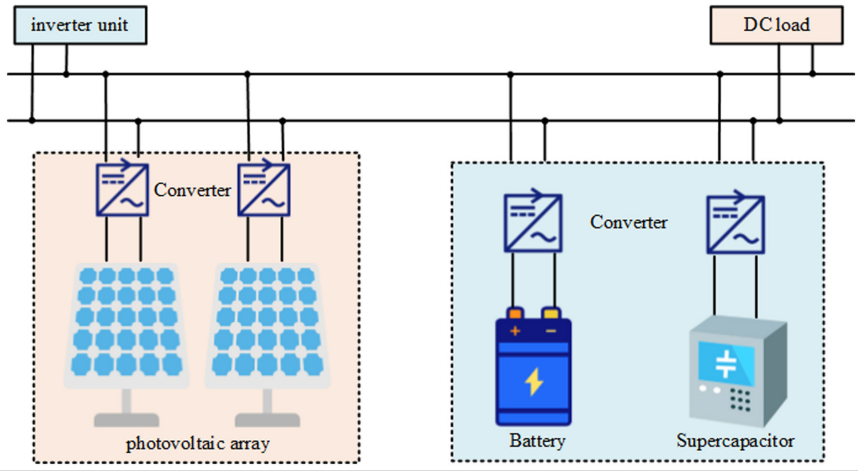

Fig. 3. Distribution network structure based on photovoltaic power source hybrid energy storage.

the independent control characteristics of two types of ES devices while achieving power-coordinated allocation through a central controller. The hybrid ES system is connected to the Alternating Current (AC) bus of the distribution network through a unified interface, forming a complementary operating mode with the photovoltaic system.

B. Capacity Configuration Optimization-Based on Dual-Layer Optical Storage

Although the power grid's stability can be enhanced and energy allocation optimized through a distribution network structure based on PP and hybrid ES, further harnessing the potential of ES systems necessitates achieving more granular energy management and efficient system operation. Therefore, the configuration of dual-layer ES needed to be optimized. Simply put, the optimization of dual-layer ES is a coordinated optimization problem that involves two levels of optimization decision-making processes, each with its own optimization objectives and constraints, as shown in (8).

$$\begin{cases} \min_{\theta, x_\theta} F(x_\theta, \theta) \\ s.t. x_\theta \in \min_x L(x, \theta) \end{cases} \tag{8}$$

In (8), x and θ represent the variables of the internal and external functions. The purpose of the internal variables is to optimize the objective function, while the external variables are to optimize the external function. F and L represent objective functions of the external and internal optimization problems, respectively. Based on this, to coordinate the interests of multiple parties and control the cost of the distribution network, a dual-layer capacity configuration optimization model was constructed, as represented in Fig. 4.

Fig. 4 shows a dual-layer capacity configuration optimization model constructed to coordinate the interests of multiple parties and consider the economic feasibility of the distribution network. From the figure, the dual-layer of the model specifically refers to the optimization model consisting of an upper layer and a lower layer. The primary goal of the UL optimization model is to minimize the operating costs of the power grid, so the service electricity price is selected as the decision variable [15, 16]. The primary goal of the LL optimization model is to minimize the operating cost of the PP station as much as possible, so the ES charging and discharging power is selected as the decision variable of the model [17]. Based on this, the objective function and constraints of the UL optimization model can be set. The objective function can be seen in (9).

$$\begin{cases} \min C = C_{pur} + C_{FM} + C_{PR} \\ C_{pur} = \sum_{t=1}^{T} \omega_{tr\_price,t} P_{grid,t} + (\omega_{DG,t} - \omega_{p,t}) P_{DG,t} \\ C_{FM} = \sum_{t=1}^{T} (\omega_{cap,t} + m\omega_{per,t}) P_{ESS,FM,t} \\ C_{PR} = \sum_{t=1}^{T} (\omega_{tr\_price,t} + \omega_{PR,t}) P_{ESS,PR,t} \end{cases} \tag{9}$$

In (9), $P_{ESS,FM,t}$ is the peak shaving power of ES, m is the mileage coefficient, min C represents the lowest electricity price, $P_{grid,t}$ represents the UL purchasing power, and C_{pur} represents the purchasing cost of electricity. C_{FM} represents frequency regulation cost, C_{PR} represents peak shaving cost, and $\omega_{tr\_price,t}$ represents time of use electricity price. $\omega_{DG,t}$ refers to the compensation electricity price for new energy, $\omega_{p,t}$ is the online fee for new energy output, P_{DG},t is the purchase power, and $\omega_{cap,t}$ is the compensation price for frequency regulation capacity. $\omega_{per,t}$ is the compensation price for frequency regulation mileage,

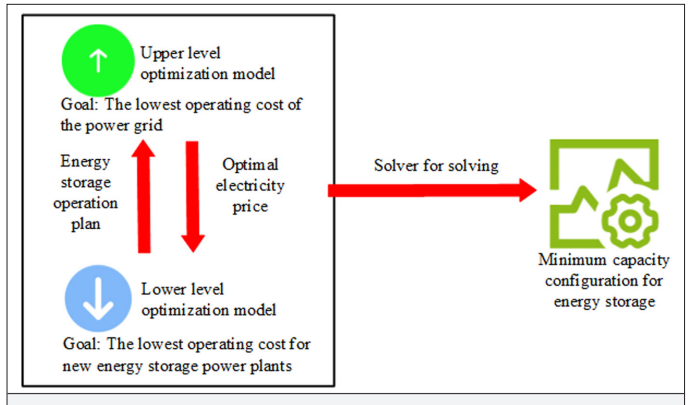

Fig. 4. Optimization model for double-layer capacity configuration.

$P_{ESS,FM,t}$ is the ES frequency regulation power, and $\omega_{PR,t}$ is the dynamic electricity price compensation for peak shaving. The upper constraint condition is (10).

$$\begin{cases} P_{grid,t} + P_{DG,t} + P_{ESS,FM,t} + P_{ESS,PR,t} = P_{L,t} \\ P_{grid,min} \le P_{grid,t} \le P_{grid,max} \\ P_{DG,min} \le P_{DG,t} \le P_{DG,max} \end{cases} \tag{10}$$

In (10), $P_{grid,t}$ represents the power of the power grid, and $P_{DG,t}$ is the power of new energy. Based on this, the UL model can be solved, and the specific process can be seen in Fig. 5.

Fig. 5 shows the solution process of the upper optimization model in the dual-layer capacity configuration model. From the figure, the process is roughly as follows: First, the initial electricity price and parameters are input into the UL model of the power grid to construct a dynamic pricing mechanism, and then the CPLEX Optimizer (CPLEX) is used to solve it, finally obtaining the most economical solution for the dynamic electricity price and UL optimization model [18, 19]. In addition, the objective function of the LL optimization model can be seen in (11).

$$\min F_{DG,ESS} = C_{total} - F_{DG} - F_{FM} - F_{PR} - F_{recyle} \tag{11}$$

In (11), C_{total} represents the total cost of ES throughout its entire life cycle. F_{PR} represents peak shaving benefits. It pertains to the advantages gained by all grid participants on both the generation and consumption sides by offering supplementary services such as frequency regulation and peak shaving, beyond basic load adjustments, to ensure grid stability. F_{FM} is the frequency modulation revenue. It refers to the revenue generated by adjusting the frequency to obtain and propagate signals. $F_{recycle}$ represents the recycling revenue, F_{DG} represents the new energy revenue, and $\min F_{DG,ESS}$ represents the objective function of minimizing the operating cost of the storage power station. The specific calculation of these benefits and costs can be seen in (12).

$$\begin{cases} C_{total} = (C_{invest} + C_{maintain} + C_{scrap})C_r \\ F_{DG} = \sum_{t=1}^{T} (\omega_{DG,t} - \omega_{p,t}) P_{DG,t} \\ F_{FM} = \sum_{t=1}^{T} (\omega_{cap,t} + m\omega_{per,t}) P_{ESS,FM,t} \\ F_{PR} = \sum_{t=1}^{T} (\omega_{tr_price,t} + \omega_{PR,t}) P_{ESS,PR,t} \\ F_{recyle} = \sum_{i=1}^{n} (R_{material_i} \gamma_{material_i} Q_N / \delta_{material_i}) C_r \end{cases} \tag{12}$$

In (12), $R_{material_i}$ represents the price of recycling waste batteries, C_{scrap} represents the cost of decommissioning and disposal, C_{invest} represents the initial input cost, $\delta_{material_i}$ represents the energy-to-weight ratio of metals in the battery, $C_{maintain}$ represents the maintenance cost, and C_r represents the constant daily coefficient. $\gamma_{material_i}$ is the metal content in waste batteries [20]. In addition, the power constraint in the constraint conditions of the LL optimization model is (13).

$$\begin{cases} 0 \le P_{FM_d,t} \le k_{FM_d,t} P_{max} \\ 0 \le P_{FM_c,t} \le k_{FM_c,t} P_{max} \\ 0 \le P_{PR,t} \le k_{PR,t} P_{max} \\ k_{FM_d,t} + k_{FM_c,t} + k_{PR,t} \le 1 \\ k_{FM_d,t} + k_{FM_c,t} + k_{PR,t} \in \{0,1\} \end{cases} \tag{13}$$

In (13), $k_{FM_c,t}$ is the frequency regulation discharge flag of the ES system, P_{max} represents the maximum power, and $k_{FM_c,t}$ is the frequency regulation charging flag of the ES system. The capacity constraint of the LL optimization model can be seen in (14).

$$\begin{cases} Q_{t+1}^{ESS} = Q_t^{ESS} + (\eta_{ch} P_{CH,t}^{ESS} - P_{DC,t}^{ESS} / \eta_{dc}) \Delta t \\ Q_{min}^{ESS} \le Q_t^{ESS} Q_{max}^{ESS} \\ Q_0^{ESS} = Q_{T_{end}}^{ESS} \end{cases} \tag{14}$$

In (14), Q_t^{ESS} represents ES capacity, Q_0^{ESS} denotes the starting value of ES capacity, and $Q_{T_{end}}^{ESS}$ represents the ending value of ES capacity. η_{ch} is the ES charging efficiency, η_{dc} is the ES discharging efficiency. Grounded on the above, the solution of the LL optimization model can be achieved, and the specific process can be seen in Fig. 6.

Fig. 6 shows the solution process of the LL optimization model. From the figure, the process first takes the dynamic electricity price obtained from the UL model as the parameter input and then solves the model to obtain the required planning results. Next, the objective function is calculated, and it is determined whether the predefined stopping criterion has been fulfilled. If met, the optimal solution is determined, and the configuration plan is output. If not, the process returns to the UL optimization model, continuing to establish a dynamic pricing mechanism grounded on the ES charging and discharging plan until the conditions are satisfied, whereupon the optimal configuration is output. Based on the above, by combining the UL optimization model and the LL optimization model, a dual-layer capacity configuration optimization model can be constructed to achieve efficient management of the distribution network, as shown in Fig. 7.

III. RESULTS

A. Experimental Platform

The simulation platform used RT-LAB OP5600 real-time simulator (CPU: Intel Xeon E5-2687W v4, FPGA: Xilinx Kintex-7) to run the model and constructed the algorithm through MATLAB/Simulink R2021a. The key simulation parameters included: power electronic device switching frequency of 10 kHz, simulation step size of 50 μs (electromagnetic transient), and 1s (electromechanical transient) dual time scale coupling. The model validation adopted the OPAL-RT HIL testing scheme, and the voltage and current measurement accuracy reached 0.1% FS. The experimental platform, as shown in Fig. 8, included: (a) a 100 kW photovoltaic array; (b) 50 kW/100 kWh lithium battery super-capacitor hybrid ES system; (c) RT-LAB OP5600 real-time simulation platform; (d) Fluke 435 Power Quality Analyzer. All devices were connected via industrial Ethernet with a sampling frequency of 10 kHz. The experimental platform was deployed in the

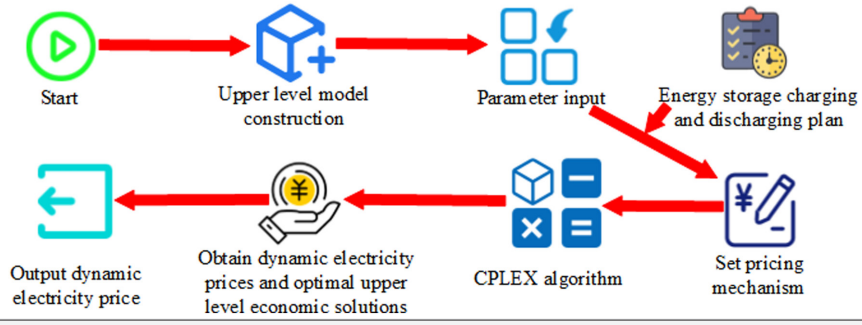

Fig. 5. The solution process of the upper level model.

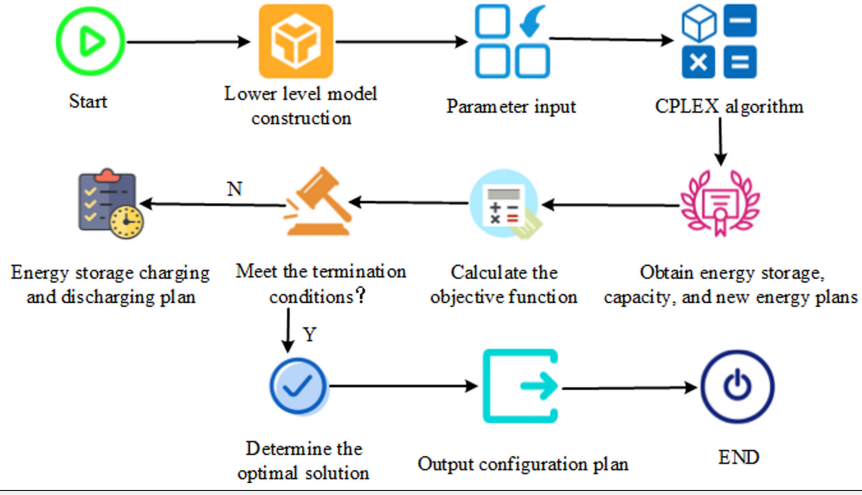

Fig. 6. The solution process of the lower level optimization model.

smart grid laboratory of a certain university and complies with the IEC 61850-7-420 standard.

The benchmark test referred to the IEEE 1547-2018 standard and set three typical scenarios: (1) Photovoltaic sag (100% to 20% step change); (2) Load impact (step from 0.5 pu to 1.5pu); (3) Continuous fluctuation (wind wave dynamic spectrum in accordance with IEC 61400-21). The testing duration was 24 hours, and the ambient temperature was controlled at 25 ± 2°C. The performance indicators were calculated using the sliding window method (window width of 10 minutes, overlap rate of 50%), and all data were collected through the Fluke 435 power quality analyzer.

B. Case Study Analysis of Hybrid Energy Storage Configuration Optimization Model for Distribution Networks with Photovoltaic Power Sources

To test the capability of the research model, a PP station was selected as the experimental object point in two provinces and cities in China, both of which have a PP of 100 kW. The study collected the power grid data of the location as experimental data for case analysis, and named the data of these two locations "A" and "B," respectively. A was a subtropical monsoon climate zone located at 31.2° N latitude, with an average annual light intensity of 580 W/m^2. B was a temperate continental climate zone located at 39.9° N latitude, with an average annual light intensity of 480 W/m^2. Both distribution networks in the two locations had a voltage level of 10 kV, but the length of the A ground feeder was 15% shorter than that of the B ground. The peak-to-valley ratio of daily load in A area was 2.8:1, with typical industrial load accounting for 65%. The peak-to-valley ratio of B was 3.5:1, with commercial load accounting for 58%. The sampling interval for load data was 1 minute, lasting for 1 year. The installed photovoltaic capacity of A site accounted for 32% of the maximum load, while B site accounted for 25%. The permeability calculation adopted the IEC 61850-7-420 standard, considering a ± 5% voltage fluctuation constraint. The testing cycle included typical days of the four seasons (vernal equinox, summer solstice, autumnal equinox, winter solstice) and extreme weather days (rainy, sandy, etc.) to ensure that the data had a certain representativeness. To present the performance of the model designed by the research more intuitively, the experiment named the research model "Photovoltaic-Hybrid ES" and compared it with traditional pumped storage-based distribution networks without photovoltaics, "Hybrid ES," and "Photovoltaic-Single ES." The study first tested the ES efficiency of each model, and the outcomes are in Fig. 9.

Fig. 9 shows the ES efficiency of the distribution network under different configurations. Fig. 9 (a) shows the ES performance in location A. From the figure, the charging efficiency of the traditional pumped storage-based distribution network was only 77.6%, which was lower than the charging efficiency of 83.2% for hybrid ES and 85.1% for single ES with PP sources. By comparison, it can be concluded that the charging efficiency of the hybrid ES system with PP supply set up by the research was the highest, at 90.1%. In terms of discharge efficiency, the traditional distribution network based

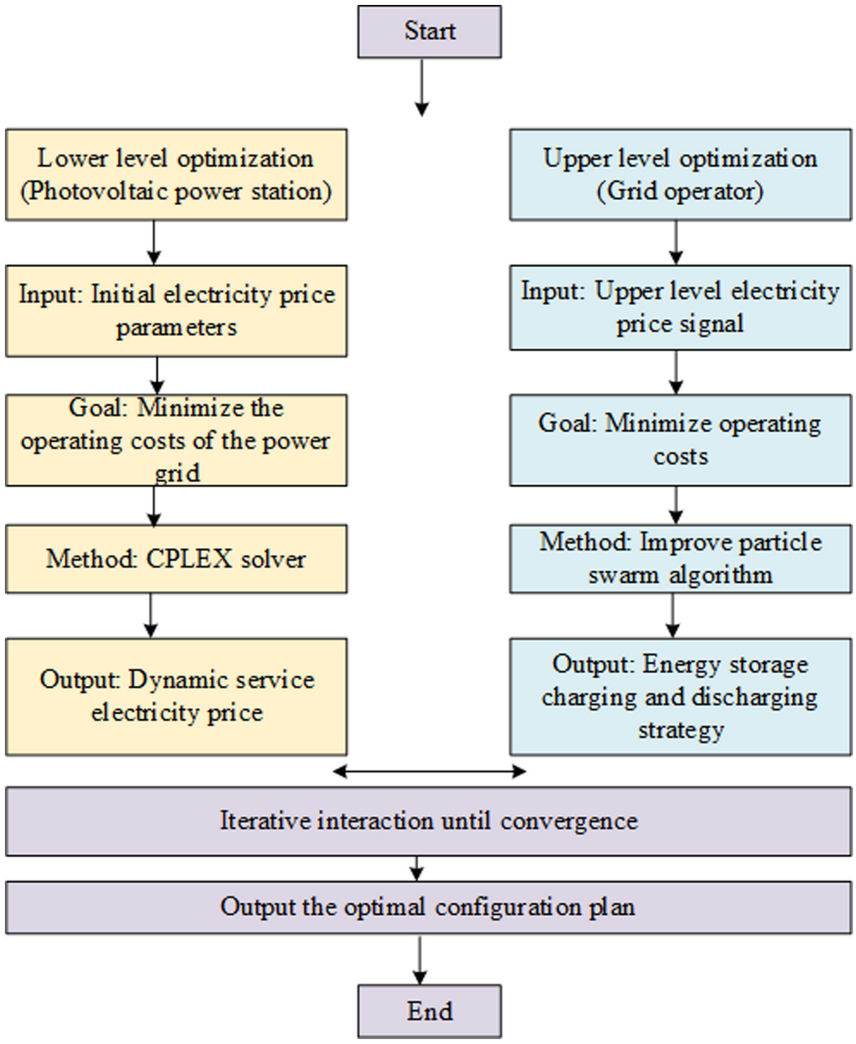

Fig. 7. Double layer capacity configuration optimization model.

on pumped storage had a discharge efficiency of 75.7%, which was lower than the discharge efficiency of 81.4% for hybrid ES and 82.1% for single ES with PP sources. By comparison, it can be concluded that the discharge efficiency of the PP source hybrid ES system set up by the research was the highest, at 91.2%. Fig. 9 (b) shows the ES performance in location B. From the graph, the charging efficiency of traditional pumped storage-based distribution networks was 78.1%, which was lower than the charging efficiency of hybrid ES at 84.8% and the charging efficiency of PP source single ES at 86.2%. By comparison, it can be concluded that the charging efficiency of the

Fig. 8. Simulation system device diagram.

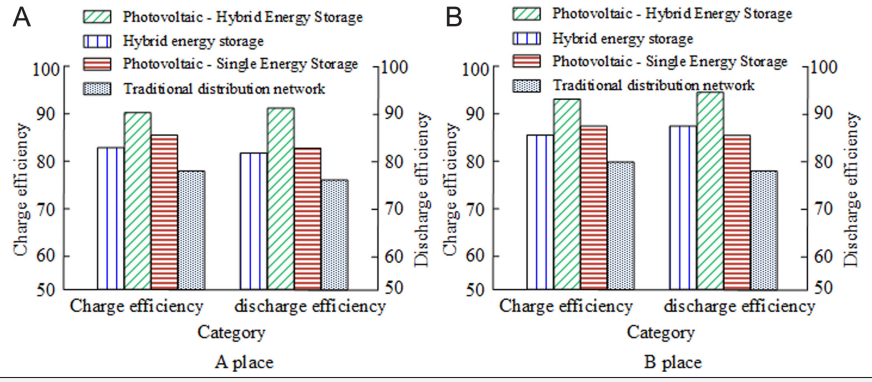

Fig. 9. Energy storage efficiency situation.

hybrid ES system with PP supply set up by the research was the highest, at 92.3%. In terms of discharge efficiency, the traditional distribution network based on pumped storage had a discharge efficiency of 76.3%, which was lower than the discharge efficiency of 87.2% for hybrid ES and 85.8% for single ES with PP sources. However, in comparison, the discharge efficiency of hybrid ES with a PP source was the highest, at 93.5%. The experiment also tested the response speed to power fluctuations in the power grid under the above configuration, and the results are shown in Fig. 10.

Fig. 10 shows the response speed of the distribution network under different configurations. Fig. 10 (a) indicates the specific performance in location A. From the figure, the traditional pumped storage-based distribution network required a response time of 5.1 seconds after receiving power fluctuation signals, which was higher than the 3.4 seconds response time of hybrid ES and the 4.1 seconds response time of single ES with PP sources. By comparison, it can be concluded that the response time of the hybrid ES system with PP supply set by the research was the lowest, at 2.9 seconds. Fig. 10 (b) shows the specific performance in location B. From the figure, the traditional pumped storage-based distribution network required a response time of 5.2 seconds after receiving power fluctuation signals, which was higher than the 4.1 seconds response time of hybrid ES and the 4.3 seconds response time of single ES with PP sources. By comparison, it can be concluded that the response time of the hybrid ES system with PP supply set by the research was the lowest, at 3.1 seconds. The shorter the response time required after receiving power fluctuation signals, the faster the response speed of the smart grid under this configuration. Therefore, overall, the model proposed by the research had the fastest speed. Furthermore, the study also examined the power smoothing effect of the power grid, as shown in Fig. 11.

Fig. 11 shows the power smoothing performance of distribution networks under different configurations. Among them, Fig. 11 (a) shows the specific manifestation in location A. From the figure, the black line represents the fluctuation of the output power of the original traditional power grid. Due to the lack of improvement in the original power grid and environmental factors such as lighting, the image had obvious fluctuations. Among the remaining three models, the configuration models based on "Hybrid ES" and "Photovoltaic-Single ES" still have a certain degree of fluctuation in output power. In contrast, the output power of the "Photovoltaic-Hybrid ES" configuration optimization model proposed by the research had the smallest degree of curve fluctuation and the best power smoothing effect. Fig. 11 (b) shows the specific performance in location B. Similar to Fig. 11 (a), in location B, the output power curve of the "Photovoltaic-Hybrid ES" proposed by the research was smoother, indicating that, under this configuration, the output power was more stable and less susceptible to environmental factors.

Further experiments also selected three typical existing methods as comparison models for secondary testing. The comparative models included traditional single-layer optimization methods, rule-based

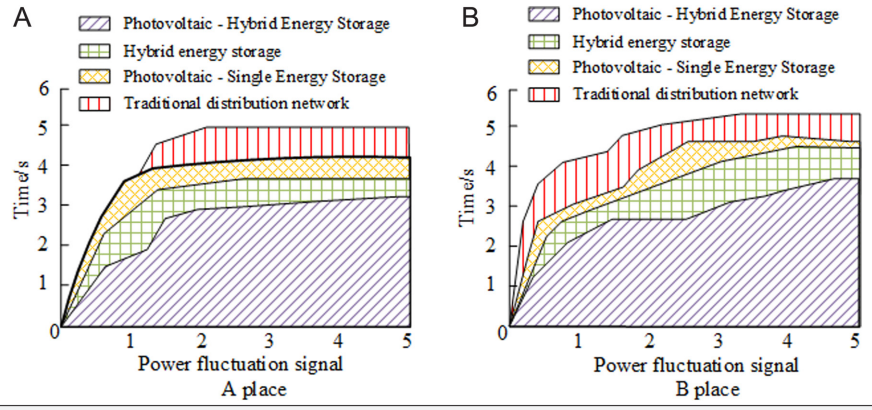

Fig. 10. Response speed situation.

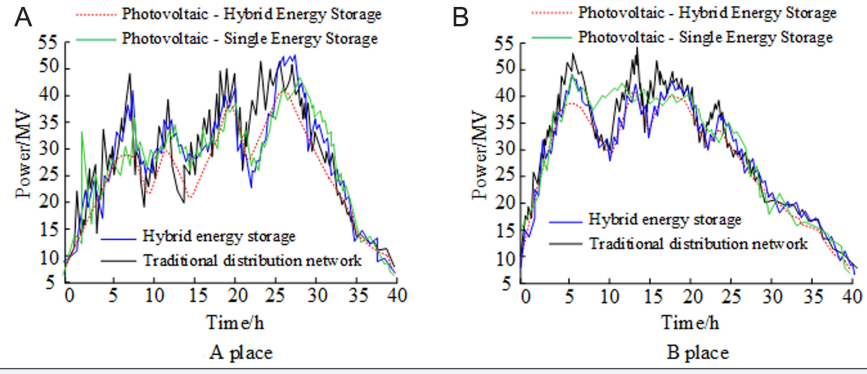

Fig. 11. Performance of power smoothing effect.

hybrid ES strategies, and distributed photovoltaic ES configuration schemes. The comparative indicators covered four key performance indicators: charging efficiency, response time, power smoothness (SD of volatility), and annual revenue per unit capacity. The test data were all from the annual operating records of the same PP station in location A. The specific comparison results are shown in Table 1.

Table 1 shows the performance comparison of different methods. From the table, the proposed model exhibited significant advantages in all key performance indicators. In terms of charging efficiency, the research model reached 90.1 ± 1.6%, which was 1.8 percentage points higher than the distributed photovoltaic ES scheme (88.3 ± 2.5%). In terms of response time, the research model only required 2.9 ± 0.4 seconds, which was 23.7% shorter than the rule-based hybrid ES strategy (3.8 ± 0.7 seconds). The primary reason for this advantage lies in the synergistic interplay between the supercapacitors' rapid response capabilities and the optimized control strategies employed. A standout aspect of this was the exceptional performance in terms of power smoothness. The SD of the research model was only 5.3 ± 1.8 W/Hz, which was 57.3% better than the traditional single-layer optimization method (12.4 ± 4.1 W/Hz), fully verifying the effective suppression ability of hybrid ES systems on photovoltaic output fluctuations. In terms of economic indicators, the annual return per unit capacity of the research model reached 225.9 yuan/kWh, which was 11.2% higher than the sub-optimal rule control strategy (203.2 yuan/kWh), mainly due to the optimization effect of the dynamic electricity pricing mechanism.

Through comparison, it can be found that although the distributed scheme performed well in charging efficiency, its power smoothness performance was the worst (15.6 ± 5.3 W/Hz), which was directly related to the lack of coordination caused by its decentralized control architecture. In contrast, the centralized hybrid ES configuration adopted in the study achieved a better balance between technical performance and economy through the collaborative optimization of lithium batteries and super-capacitors.

C. Example Analysis of Hybrid Energy Storage Configuration Optimization Model for Distribution Networks with Photovoltaic Power Sources

Due to the fact that the above experiment only examined the specific performance of each model, to further observe the performance of the research model in practical operation, the study proposed to conduct an example analysis on this. The study took a certain energy field in location C of a certain province and city as the experimental object, selected typical days during the actual operation of the station, and obtained the time of use electricity price of the area. Then, through the joint optimization of the upper and lower layers of the dual-layer capacity configuration optimization model set by the research, the output power under the dynamic service electricity price and fixed electricity price mechanism was calculated. The results are shown in Fig. 12.

Fig. 12 shows the power output curve under the service electricity price and fixed electricity price mechanisms. Fig. 12 (a) indicates the power output under the service pricing mechanism. From the graph, it can be seen that during the periods of 10:00–11:00 and 20:00–21:00, the ES was discharged at full power, indicating that this period was the peak period of electricity consumption. At 9:00, 17:00–18:00, and 23:00, the ES was still discharged at full power, but the intensity was slightly weaker than at 10:00–11:00 and 20:00–21:00, indicating a peak period of electricity consumption. At 3:00–4:00, 12:00–16:00, and 19:00, the power decreased, and charging was carried out during this time of registration. Fig. 12 (b) shows the output power under the fixed electricity price mechanism. From the figure, under the fixed electricity price mechanism, the peak periods of electricity consumption were from 9:00 to 10:00 and from 17:00 to 18:00, while the sub-peak periods were at 11:00, 19:00, 21:00, and 23:00.

TABLE I. PERFORMANCE COMPARISON OF DIFFERENT METHODS

Metric	Single-Layer	Rule-Based HES	Distributed	Proposed Model
Charging efficiency (%)	82.1 ± 3.2	85.7 ± 2.8	88.3 ± 2.5	90.1 ± 1.6
Response time (s)	4.7 ± 0.9	3.8 ± 0.7	5.2 ± 1.1	2.9 ± 0.4
Power smoothness (W/Hz)	12.4 ± 4.1	8.7 ± 3.2	15.6 ± 5.3	5.3 ± 1.8
Annual revenue (RMB/kWh)	186.5	203.2	175.8	225.9

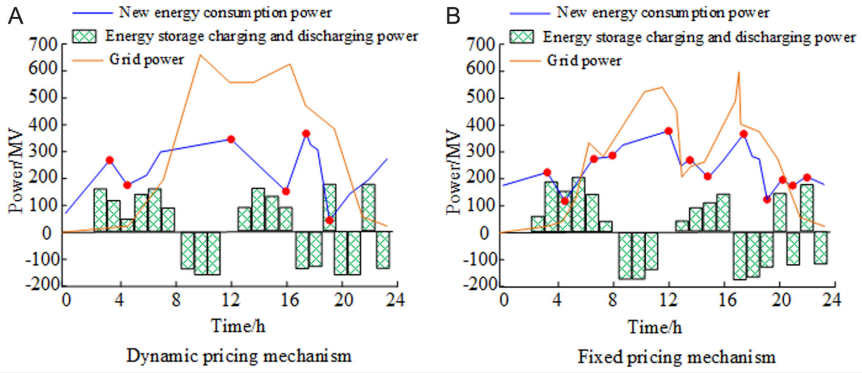

Fig. 12. Output power under service electricity price and fixed electricity price mechanism.

Although there were differences in the times for ES to discharge at full power under different pricing mechanisms, the research model could still guide ES to discharge at full power during the highest peak, maximizing revenue. Further experiments also calculated the comparison of load before and after configuring ES under these two mechanisms, as shown in Fig. 13.

Fig. 13 shows the comparison of load before and after configuring ES under different pricing mechanisms. Fig. 13 (a) shows the comparison of pre and post load of ES configuration under the dynamic tiered service pricing mechanism. From the graph, when ES was not configured, the highest peak power in the original load curve was 1021.4 kW, the lowest power was 102.8 kW, and the peak valley difference was 918.6 kW. After configuring ES, the peak valley difference was 698.8 kW, which was lower compared to before configuration. Based on this, it can be proven that the proposed model could effectively guide ES to participate in peak shaving and reduce the load peak valley difference under a dynamic electricity pricing mechanism. Fig. 13 (b) shows the comparison of pre and post load of ES configuration under a fixed electricity pricing mechanism. From the graph, when ES was not configured, the highest peak power in the original load curve was 1105.2 kW, the lowest power was 102.1 kW, and the peak valley difference was 1003.1 kW. After configuring ES, the peak valley difference of the equivalent load decreased to 813.2 kW. This indicated that the model proposed by the research could also guide ES to regulate the initial load to a certain extent under the fixed price mechanism, and also participate in frequency regulation services. Furthermore, the experiment conducted a profit analysis under these two electricity pricing systems, and the outcomes are in Table 2.

Table 2 shows the revenue situation of the research model under different pricing mechanisms. From the table, under dynamic mechanisms, the cost of optimizing the UL model for ES was higher and higher than that of the UL model under fixed mechanisms. However, in terms of purchasing electricity cost, the purchasing cost of ES under the dynamic mechanism was 8567.5 yuan, which was lower than the purchasing cost under the fixed mechanism. Furthermore, in terms of total returns, the model had the highest returns under dynamic mechanisms. This indicates that under the dynamic electricity pricing mechanism, it is more economical.

IV. DISCUSSION

To raise the automation level of the distribution network, enhance work efficiency, and promote the rapid development of the distribution network, this study proposed the introduction of PP sources and hybrid ES technology to construct a configuration model for the power grid, and based on this, conducts dual-layer capacity configuration to optimize the model. To test the generalization ability of the model, the power grids of A and B were used as experimental objects for testing. The experimental results showed that in terms of ES efficiency, the hybrid ES model with PP supply set up by the research had the highest charging and discharging efficiency in location A compared to other models, with a charging efficiency of 90.1% and a discharging efficiency of 91.2%. In location B, the charging efficiency

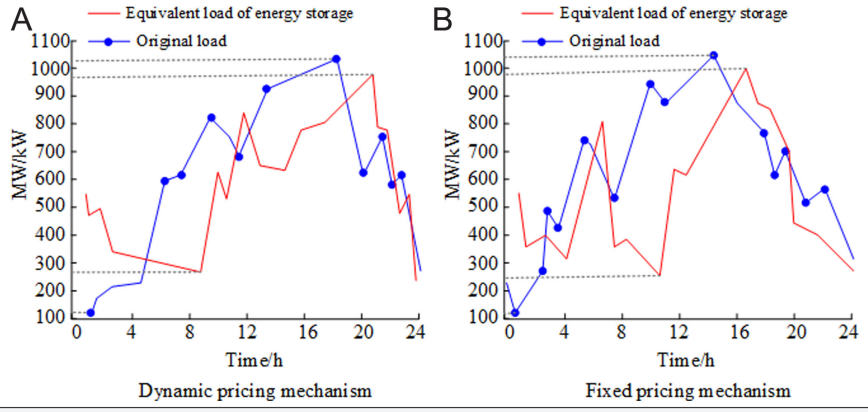

Fig. 13. Comparison of pre and post load of energy storage configuration under different pricing mechanisms.

TABLE II. REVENUE UNDER VARIOUS PRICING MECHANISMS

	Dynamic Electricity Price	Fixed Electricity Price
ES capacity	500 kwh	500 kwh
Upper level cost (UL)	12862.1 rmb	10567.5 rmb
Lower level cost (LL)	−10876.5 rmb	−13657.4 rmb
Electricity purchasing cost	8567.5 rmb	20341.4 rmb
Net proceeds	112987.1 rmb	78968.6 rmb
Peak shaving revenue	1043.5 rmb	768.6 rmb
FM revenue	489.6 rmb	409.2 rmb

FM, Frequency Modulation.

reached 92.3% and the discharging efficiency reached 93.5%. In terms of response speed, the calculation results of A and B sites showed that the response time of the PP source hybrid ES set by the research was the lowest compared to other models, which were 2.9 s and 3.1 s respectively, indicating that the smart grid response speed under the configuration set by the research was faster. In terms of the power smoothing effect, regardless of whether it was in location A or B, the output power of the proposed model had the least fluctuation in its curve and the best power smoothing effect. In the case analysis, the output power of the model was calculated under dynamic service pricing and fixed pricing mechanisms. As a result, it was found that regardless of the pricing mechanism, the research model could guide ES to discharge at full power during the highest peak, maximizing revenue. In addition, by comparing the load before and after configuring ES, it was found that the model could effectively guide ES to participate in peak shaving and reduce the load peak valley difference, whether under a dynamic electricity pricing mechanism or fixed electricity pricing mechanism. However, from the perspective of cost expenditure, under the mechanism of dynamic electricity prices, this model had stronger participation in ES services and higher returns. Compared with research in the same field, Vijayan et al. developed a stochastic optimization equation to solve the problems of peak demand, energy loss, and system-wide imbalance in modern three-phase active distribution networks [21]. The experiment outcomes showed that compared with traditional collaborative optimization methods, this method not only provides an effective solution but also reduces time by 75%. Kalaiselvan et al. proposed using a coordinated approach to integrate energy, combining solar photovoltaics and small-scale hydropower, and introducing microgrid systems, in order to ensure productivity and minimize problems [22]. The experimental results showed that this technology provided lower power loss than existing methods, with an average value of 1.0935. However, compared to the effects presented by the research model, the model designed by the research performed better overall.

V. CONCLUSION

To raise the automation level of the distribution network, enhance work efficiency, and promote the rapid development of the distribution network, this study proposes the introduction of PP sources and hybrid ES technology to construct a configuration model for the power grid, and based on this, conducts dual-layer capacity configuration to optimize the model. The experimental outcomes indicated that in the case analysis, the proposed model achieved a charging efficiency of 90.1% and a discharging efficiency of 91.2% in location A. In location B, the charging efficiency of this model reached 92.3% and the discharging efficiency reached 93.5%, both of which were superior to other comparative models, indicating good ES efficiency. In addition, the model had the best response time of 2.9 s and 3.1 s in two locations A and B, respectively, and its power smoothing effect also had good performance. In the case analysis, the experiment outcomes indicated that the model could guide ES to discharge at full power during the highest peak and participate in peak shaving, reducing the load peak valley difference and maximizing profits. Although research achieved certain results, the intermittency and randomness of PP generation can easily bring great uncertainty to the capacity configuration of hybrid ES systems. Therefore, future research can attempt to integrate multiple prediction techniques, such as combining physics-based mathematical models of photovoltaic cells with statistical analysis methods based on historical data, to further optimize and enhance the reliability of the configuration.

Data Availability Statement: The data that support the findings of this study are available on request from the corresponding author.

Peer-review: Externally peer-reviewed.

Author Contributions: Concept – X.H., D.X.; Design – X.H., D.X; Supervision – D.X., X.T.; Resources – X.T.; Materials – X.H., X.T.; Data Collection and/or Processing – X.H.; Analysis and/or Interpretation – X.H., X.T.; Literature Search – X.Q.; Writing – X.H., D.X., X.Q., X.T.; Critical Review – X.H., X.H., X.Q.

Declaration of Interests: The authors have no conflicts of interest to declare.

Funding: The authors declare that this study received no financial support.

REFERENCES

1. K. E. Bassey, "Hybrid renewable energy systems modeling," *Eng. Sci. Technol. J.*, vol. 4, no. 6, pp. 571–588, 2023. [CrossRef]
2. M. Amir, A. Zaheeruddin Haque, A. Haque, F. I. Bakhsh, V. S. B. Kurukuru, and M. Sedighizadeh, "Intelligent energy management scheme-based coordinated control for reducing peak load in grid-connected photovoltaic-powered electric vehicle charging stations," *IET Generation Trans. & Dist.*, vol. 18, no. 6, pp. 1205–1222, 2024. [CrossRef]
3. K. Gupta, R. Achathuparambil Narayanankutty, K. Sundaramoorthy, and A. Sankar, "Optimal location identification for aggregated charging of electric vehicles in solar photovoltaic powered microgrids with reduced distribution losses," *Energy Sources A*, vol. 46, no. 1, pp. 6289–6304, 2024. [CrossRef]
4. K. Liu et al., "An energy optimal schedule method for distribution network considering the access of distributed generation and energy storage," *IET Generation Trans. & Dist.*, vol. 17, no. 13, pp. 2996–3015, 2023. [CrossRef]
5. W. Anupong et al., "Deep learning algorithms were used to generate photovoltaic renewable energy in saline water analysis via an oxidation process," *Water Reuse*, vol. 13, no. 1, pp. 68–81, 2023. [CrossRef]
6. Q. Yang, X. Chen, H. Wang, P. Jia, Z. Yue, and M. Yao, "Configuration planning and operation strategy of off-grid wind solar storage hybrid energy system based on hydrogen fuel energy storage," *J. Combust. Sci. Technol.*, vol. 31, no. 2, pp. 138–149, 2025.
7. M. Z. A. Bhatti, A. Siddique, W. Aslam, and S. Atiq, "Design and analysis of a hybrid stand-alone microgrid," *Energies*, vol. 17, no. 1, p. 200, 2023. [CrossRef]
8. Y. Wang, W. Fu, X. Zhang, Z. Zhen, and F. Wang, "Dynamic directed graph convolution network based ultra-short-term forecasting method of distributed photovoltaic power to enhance the resilience and flexibility of distribution network," *IET Generation Trans. & Dist.*, vol. 18, no. 2, pp. 337–352, 2024. [CrossRef]

9. V. Janamala, K. R. Rani, P. Sobha Rani, A. N. Venkateswarlu, and S. R. Inkollu, "Optimal switching operations of soft open points in active distribution network for handling variable penetration of photovoltaic and electric vehicles using artificial rabbits optimization," *Process Integr. Optim. Sustain.*, vol. 7, no. 1–2, pp. 419–437, 2023. [CrossRef]
10. A. Mishra, M. Tripathy, and P. Ray, "A survey on different techniques for distribution network reconfiguration," *J. Eng. Res.*, vol. 12, no. 1, pp. 173–181, 2024. [CrossRef]
11. A. R. Vadavathi, G. Hoogsteen, and J. Hurink, "PV inverter-based fair power quality control," *IEEE Trans. Smart Grid*, vol. 14, no. 5, pp. 3776–3790, 2023. [CrossRef]
12. S. M. R. H. Shawon, X. Liang, and M. Janbakhsh, "Optimal placement of distributed generation units for microgrid planning in distribution networks," *IEEE Trans. Ind. Appl.*, vol. 59, no. 3, pp. 2785–2795, 2023. [CrossRef]
13. R. Leng, Z. Li, and Y. Xu, "Two-stage stochastic programming for coordinated operation of distributed energy resources in unbalanced active distribution networks with diverse correlated uncertainties," *J. Mod. Power Syst. Clean Energy*, vol. 11, no. 1, pp. 120–131, 2023. [CrossRef]
14. H. Lotfi, and A. A. Shojaei, "A dynamic model for multi-objective feeder reconfiguration in distribution network considering demand response program," *Energy Syst.*, vol. 14, no. 4, pp. 1051–1080, 2023. [CrossRef]
15. S. S. Dheeban, and N. B. Muthu Selvan, "ANFIS-based power quality improvement by photovoltaic integrated UPQC at distribution system," *IETE J. Res.*, vol. 69, no. 5, pp. 2353–2371, 2023. [CrossRef]
16. V. Gopu, and M. S. Nagaraj, "Power management algorithm for standalone operated renewable distribution generator with hybrid energy backup in microgrid," *IJPEDS*, vol. 14, no. 2, pp. 1249–1259, 2023. [CrossRef]
17. X. Yang et al., "Network-constrained transactive control for multi-microgrids-based distribution networks with soft open points," *IEEE Trans. Sustain. Energy*, vol. 14, no. 3, pp. 1769–1783, 2023. [CrossRef]
18. A. Pal, A. Bhattacharya, and A. K. Chakraborty, "Planning of EV charging station with distribution network expansion considering traffic congestion and uncertainties," *IEEE Trans. Ind. Appl.*, vol. 59, no. 3, pp. 3810–3825, 2023. [CrossRef]
19. Y. Qiao, F. Hu, W. Xiong, and Y. Li, "Energy hub-based configuration optimization method of integrated energy system," *Int. J. Energy Res.*, vol. 46, no. 15, pp. 23287–23309, 2022. [CrossRef]
20. P. P. Groumpos, "A critical historic overview of artificial intelligence: Issues, challenges, opportunities, and threats," *Artif. Intell. Appl.*, vol. 1, no. 4, pp. 181–197, 2023. [CrossRef]
21. V. Vijayan, A. Mohapatra, S. N. Singh, and C. L. Dewangan, "An efficient modular optimization scheme for unbalanced active distribution networks with uncertain EV and PV penetrations," *IEEE Trans. Smart Grid*, vol. 14, no. 5, pp. 3876–3888, 2023. [CrossRef]
22. K. Kalaiselvan, R. Saravanan, B. Adhavan, and G. S. Manikandan, "Hybrid methodology-based energy management of microgrid with grid-isolated electric vehicle charging system in smart distribution network," *Electr. Eng.*, vol. 106, no. 3, pp. 2705–2720, 2024. [CrossRef]

Xinping Huang was born in September 1981 in Xiushui County, Jiangxi Province, China. He received the B.Eng. degree in electrical power systems engineering from the Department of Civil Engineering, Northeast Electric Power University, Jilin City, China, in 2004, and the M.Eng. degree in project management from the School of Economics and Management, North China Electric Power University, Beijing, China, in 2011. His research focuses on distribution network optimization with distributed photovoltaic generation, hybrid energy storage capacity allocation, and multi-energy system coupling modeling. Currently a Senior Engineer at State Grid Jibei Electric Power Company Limited, Beijing, China, he previously served as Deputy Director of the Development Department at Qinghai Electric Power Company and Jibei Electric Power Company, leading the design of multiple 100-MW-level photovoltaic grid integration systems. His research achievements include the authorized patent *Internet-based Power Supply Planning Management Method* implemented in Jibei regional grid planning, and the pending patent *Electric Load Forecasting Method, System and Computer Device* under deployment in smart grid platforms. The management innovation project *Carbon Asset Management System Construction for Power Enterprises* was awarded the 2023 Third Prize by State Grid Jibei Electric Power Company. He was honored with the Beijing May 1st Labor Medal in 2008 (issued by Beijing Municipal Trade Union Council) for outstanding contributions to Olympic Games power supply assurance. His early research pioneered structural reliability analysis of transmission projects and grid construction technology optimization.

Decao Xu, a native of Suzhou, Anhui Province, graduated with a master's degree from North China Electric Power University. He joined State Grid Qinghai Electric Power Company in May 2007. From 2010 to 2023, he engaged in power grid development work, during which he actively conducted research and engineering demonstrations to enhance new energy integration capabilities. His research on "Key Technologies for UHV AC/DC Transmission Systems with Ultra-High Proportion Renewable Energy" was awarded the Second Prize of Qinghai Provincial Science and Technology Award in 2017. Additionally, his study on "Integrated Multi-Energy Complementary Systems" received the First Prize of Qinghai Provincial Science and Technology Award in 2022.

Xuwu Qin was born in Wanzhou District, Chongqing, China in May 1983. He received a Diploma in power system and automation from Chongqing Electric Power College (Chongqing, China) in July 2004, later obtaining a Bachelor of Engineering degree in electrical engineering and automation from Sichuan University (Chengdu, China) in January 2012. Since February 2014, he has worked at the Development Planning Department of State Grid Qinghai Electric Power Company (Xining, China), progressing from Deputy Director of Transmission Grid Planning Division to Director of Investment Division and currently serving as Director of Distribution Grid Planning Division (2025-present). His expertise spans 330kV transmission project feasibility studies, renewable energy grid integration, and provincial investment statistics. Current research focuses on hybrid energy storage systems and big data-driven grid forecasting.

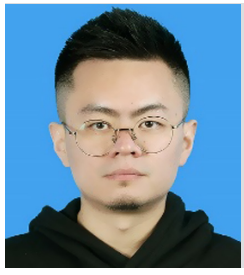

Xin Tao was born in Xining, Qinghai Province, China in September 1988. He earned a Bachelor of Engineering degree in power system and automation from North China Electric Power University (Beijing, China) in July 2012, followed by a part-time Master of Engineering degree in electrical engineering from Sichuan University (Chengdu, China) in December 2019. He joined State Grid Qinghai Electric Power Company in July 2012, serving successively at its Economic and Technical Research Institute and Development Planning Department until February 2025. His roles included Supervisor of the Planning Review Center and Investment Management Specialist, specializing in power grid planning reports, engineering feasibility studies, investment strategy formulation, and asset acquisition projects. He is proficient in power grid optimization and capital allocation systems. Current research interests focus on smart grid resilience and investment decision modeling.